Dipole-dipole interaction in a photonic crystal nanocavity

Yong-Gang Huang,[1,2] Gengyan Chen,[1] Chong-Jun Jin,[1] W. M. Liu,[2] and Xue-Hua Wang[1,*]

[1]*State Key Laboratory of Optoelectronic Materials and Technologies, Sun Yat-sen University, Guangzhou 510275, China*

[2]*Beijing National Laboratory for Condensed Matter Physics, Institute of Physics, Chinese Academy of Sciences, Beijing 100190, China*

(Received 22 January 2012; published 22 May 2012)

We put forward a general classical approach to obtain the quantum dipole-dipole interaction (DDI) between two two-level "atoms" in arbitrary nanostructures, in which the transfer rate of the DDI is analytically expressed as the difference between the two classical dipoles' total radiation power and the sum of the two individual dipole's radiation powers. The radiation power can be calculated by the finite-difference time-domain method. We apply the theory to investigate the DDI in a photonic crystal nanocavity. It is found that strong DDI at a distance can be achieved under resonant conditions and with a high quality factor, and the attractive or repulsive properties of the DDI can be manipulated. Our results should be significant for solid-state quantum-information processing based on the DDI.

DOI: 10.1103/PhysRevA.85.053827 PACS number(s): 42.50.Ct, 34.20.−b, 37.30.+i

I. INTRODUCTION

Since Purcell predicted that the spontaneous emission rate could be changed by the electromagnetic environment in 1946 [1], the effect of electromagnetic fields on radiation properties has been thoroughly investigated [2–10] and classified in the category of cavity quantum electrodynamics (QED). The characteristics of QED have been much investigated both theoretically and experimentally [11–17], and many kinds of devices [18,19] based on this theory have been developed. Concepts such as enhanced and inhibited spontaneous emission [4,5], reversible spontaneous emission [8], photon blockade [13], the one-atom maser [20], low-threshold lasers [21,22], etc., have become very familiar.

The quantum dipole-dipole interaction (DDI) could also be greatly modulated by the electromagnetic environment. Two two-level atoms with one excited and the other in the ground state can interact with each other through photon exchange. A photon emitted by the excited atom could be absorbed by the other atom in the ground state. The transfer rate and the DDI potential energy are determined by the rates of photon emission, transmission, and absorption. Many different kinds of electromagnetic environment have been used to control or change these characteristics, such as the vacuum [3,23–26], optical cavities [27–30], an optical lens [31], a dielectric droplet [32], photonic materials [33–39], metal surfaces [40–44], metamaterials [45,46], and so on. For example, optical lenses and waveguides have been designed to collect the emitted photon and transfer it to the other dipole. An optical cavity or metal surface can enhance the emission or absorption rate roughly by the ratio of the quality factor Q and the mode volume V.

Photonic crystal nanocavities are one promising platform to investigate the quantum DDI. It can tailor the local coupling strength between the dipole and electromagnetic field and is extremely convenient to integrate with the photonic crystal waveguide. A high quality factor $Q = 2.5 \times 10^6$ and small mode volume $V \sim (\lambda/n)^3$ have been realized for a photonic crystal cavity [47]. Numerical investigations show that an ultrahigh quality factor $Q \sim 10^9$ can be designed through finely tuning the scattering around the cavity with little change of the mode volume [48]. Furthermore, static and ultrafast dynamic control of the resonance frequency and the quality factor have been achieved [49–53]. On the other hand, temperature [9], tensile strain [54], electric fields [55], and magnetic fields [56,57] are more suitable for tuning the energy levels of semiconductor quantum dots located at a certain position in a solid system.

Recent studies show that this kind of interaction could be used to implement quantum entanglement preparation and quantum information processing [58–65], cooperative radiation [29,66], Förster energy transfer [67,68], dipole nanolasers [69], and so on. Furthermore, some novel quantum phenomena have been found [70–74]. All of these applications and phenomena are related to the transfer rate or DDI potential energy.

In previous theoretical studies, either the mode-expansion method [24,27,28,31–33] or the Green-function method [30,63–65,75,76] was usually adopted to obtain the transfer rate and DDI potential energy. These two methods work well for simple electromagnetic environments. Because of the extreme complexity of finding the complete eigenmodes, the mode-expansion method can be used only for simple cases such as the vacuum or a perfect-conductor planar cavity. In addition, the exact analytic Green function [63] is also very hard to obtain for complex electromagnetic environments. A numerical method is necessary for studying this kind of interaction in nanostructures with arbitrary geometry.

In this paper, we present a general classical approach to obtain the quantum DDI in nanostructures with arbitrary geometry. We analytically derive the expression of the DDI by the difference between the two classical dipoles' total radiation power and the sum of the two individual dipole's radiation powers. The radiation powers are obtained by numerically solving the Maxwell equations with a finite-difference time-domain (FDTD) algorithm. For two dipoles located in a photonic crystal nanocavity, the transfer rate and the potential energy of the DDI strongly depend on the atomic position, the atomic transition frequency, and the resonance frequency and

*Corresponding author: wangxueh@mail.sysu.edu.cn

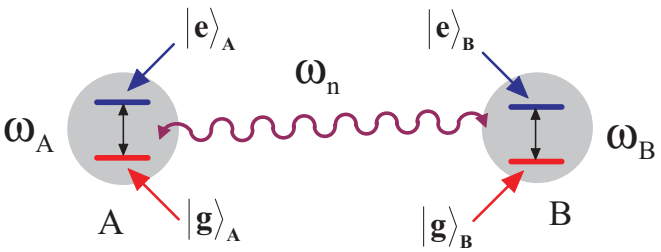

FIG. 1. (Color online) Schematic diagram of the DDI. Consider two two-level "atoms" A and B. Atom A (B) has two states, the ground state $|g_A\rangle$ ($|g_B\rangle$) and the excited state $|e_A\rangle$ ($|e_B\rangle$), with a transition frequency ω_A (ω_B). Atom A is in the excited state $|e_A\rangle$ and atom B is in the ground state $|g_B\rangle$. Both of them interact with the electromagnetic field with eigenfrequency ω_n. The two atoms interact with each other through photon exchange.

quality factor of the cavity. A fast transfer rate can be achieved if the atomic transition frequency is equal to the resonance frequency of the cavity. The higher is the quality factor of the cavity, the stronger is the DDI. By finely tuning the atomic transition frequency within the linewidth of the cavity mode around the resonance frequency, the potential energy of the DDI is varied continuously from the attractive to the repulsive case.

This paper is organized as follows: The quantum model of the DDI is given in Sec. II. In Sec. III, we propose a general classical approach to obtain the quantum DDI. Utilizing the eigenmode-expansion method, we show that the transfer rate can be analytically expressed as a function of the emission power spectrum of classical dipoles. The emission power spectrum is obtained by calculating the rate at which a current density source does work against a surrounding electric field through the FDTD algorithm without any knowledge of the eigenmodes. In Sec. IV, we apply the theory to investigate properties of the DDI in a photonic crystal nanocavity. Finally, a summary is given in Sec. V.

II. QUANTUM MODEL OF DDI BETWEEN TWO ATOMS

The schematic diagram of the DDI is illustrated in Fig. 1. There are two two-level "atoms" A and B located at $\mathbf{r}_A$ and $\mathbf{r}_B$, respectively, and they both interact with the electromagnetic field with eigenfrequency ω_n. Atom A (B) has two states, the ground state $|g_A\rangle$ ($|g_B\rangle$) and the excited state $|e_A\rangle$ ($|e_B\rangle$), with a transition frequency ω_A (ω_B). The Hamiltonian of the system in the rotating-wave approximation reads [77]

$$\begin{aligned} H &= H_0 + V, \\ H_0 &= \hbar \sum_{i=A,B} \omega_i |e_i\rangle\langle e_i| + \hbar \sum_n \omega_n a_n^\dagger a_n, \\ V &= \hbar \sum_{i=A,B} \sum_n [g_n(\mathbf{r}_i) a_n^\dagger |g_i\rangle\langle e_i| + \text{c.c}], \end{aligned} \tag{1}$$

where $a_n^\dagger$ (a_n) is the photonic creation (annihilation) operator, $g_n(\mathbf{r}_i) = i\omega_j(2\varepsilon_0\hbar\omega_n)^{-1/2}\mathbf{E}_n(\mathbf{r}_i)\cdot\mathbf{u}_i$ ($i = A,B$) is the coupling coefficient, $\mathbf{u}_i$ is the transition dipole moment of atom i, ε_0 is the vacuum permittivity, and $\mathbf{E}_n(\mathbf{r})$ is the electric field of the eigenmode. In Eq. (1), H_0 is the noninteraction Hamiltonian, and V represents the interaction Hamiltonian. There are three states for the system considered: (1) atom A is in the excited state and atom B is in the ground state, without any photon, i.e., $|a\rangle = |e_A, g_B, 0\rangle$; (2) atom B is in the excited state and atom A is in the ground state, without any photon, i.e., $|b\rangle = |g_A, e_B, 0\rangle$; (3) both atoms A and B are in the ground state, with a photon of frequency ω_n, i.e., $|c_n\rangle = |g_A, g_B, 1_n\rangle$.

The initial state is prepared in $|a\rangle$. Then the state vector of the system evolves as

$$|\psi(t)\rangle = a(t)|a\rangle + b(t)|b\rangle + \sum_n c_n(t)|c_n\rangle \equiv U(t)|a\rangle, \tag{2}$$

where $U(t)$ is the evolution operator and $a(t) = \langle a|U(t)|a\rangle$, $b(t) = \langle b|U(t)|a\rangle$, $c_n(t) = \langle c_n|U(t)|a\rangle$. From the Green-function expression of $U(t)$, one can show that [78]

$$U(t) = \frac{1}{2\pi i}\int_{-\infty}^{+\infty} d\omega [G^-(\omega) - G^+(\omega)] \exp(-i\omega t), \tag{3}$$

where $G^\pm(\omega) = \lim_{\eta\to 0^+} G(z = \omega \pm i\eta)$ with the resolvent operator $G(z) = (z - H/\hbar)^{-1}$. The matrix elements of the resolvent operator read

$$\begin{aligned} (z-\omega_A)G_{aa}(z) &= 1 + \sum_n V_{ac}G_{ca}(z), \\ (z-\omega_B)G_{ba}(z) &= \sum_n V_{bc}G_{ca}(z), \\ (z-\omega_n)G_{ca}(z) &= V_{ca}G_{aa}(z) + V_{cb}G_{ba}(z), \end{aligned} \tag{4}$$

where $G_{aa}(z) = \langle a|G(z)|a\rangle$, $G_{ba}(z) = \langle b|G(z)|a\rangle$, $G_{ca}(z) = \langle c_n|G(z)|a\rangle$ and $V_{ac} = V_{ca}^* = \langle a|V|c_n\rangle/\hbar$, $V_{bc} = V_{cb}^* = \langle b|V|c_n\rangle/\hbar$.

Eliminating $G_{ca}(z)$, we have

$$\begin{aligned} G_{aa}(z) &= (z - \omega_B - W_{BB})/\Xi, \\ G_{ba}(z) &= W_{BA}/\Xi, \end{aligned} \tag{5}$$

where Ξ is given by

$$\Xi = [z - \omega_A - W_{AA}][z - \omega_B - W_{BB}] - W_{AB}W_{BA} \tag{6}$$

with the local coupling between the atom and the electromagnetic field (W_{AA}, W_{BB}) or the dipole-dipole coupling between atoms A and B (W_{AB}, W_{BA}) denoted by

$$W_{ij} = W_{ij}(z, \mathbf{r}_i, \mathbf{r}_j) = \sum_n \frac{g_n^*(\mathbf{r}_i)g_n(\mathbf{r}_j)}{z - \omega_n}. \tag{7}$$

Clearly, these terms can be written as

$$W_{ij}^\pm(\omega, \mathbf{r}_i, \mathbf{r}_j) = \Delta_{ij}(\omega, \mathbf{r}_i, \mathbf{r}_j) \mp i\frac{\Gamma_{ij}(\omega, \mathbf{r}_i, \mathbf{r}_j)}{2}, \tag{8a}$$

$$\Gamma_{ij}(\omega, \mathbf{r}_i, \mathbf{r}_j) = 2\pi \sum_n g_n^*(\mathbf{r}_i)g_n(\mathbf{r}_j)\delta(\omega - \omega_n), \tag{8b}$$

$$\Delta_{ij}(\omega, \mathbf{r}_i, \mathbf{r}_j) = \frac{1}{2\pi}\mathrm{P}\int_0^{+\infty} dz \frac{\Gamma_{ij}(\omega', \mathbf{r}_i, \mathbf{r}_j)}{\omega - \omega'}. \tag{8c}$$

For simplicity, we use $\Gamma_{ij}(\omega)$ and $\Delta_{ij}(\omega)$ for $\Gamma_{ij}(\omega, \mathbf{r}_i, \mathbf{r}_j)$ and $\Delta_{ij}(\omega, \mathbf{r}_i, \mathbf{r}_j)$, respectively, in the remainder of this paper.

To better understand the physics underlying these equations, we give some illustrations. In the extreme case that there is no DDI between the two atoms, i.e., $\Gamma_{AB} = \Delta_{AB} = 0$, Eq. (5) gives $A_{ba}(\omega) = 0$ and $[\Gamma_{AA}(\omega)/2 + \eta]/\{[\omega - \omega_A - \Delta_{AA}(\omega)]^2 + [\Gamma_{AA}(\omega)/2 + \eta]^2\}/\pi$ with the matrix element

of the evolution spectrum defined by $A_{mn}(\omega) \equiv [G^{-}_{mn}(\omega) - G^{+}_{mn}(\omega)]/(2\pi i)$. It clearly shows that the initial excitation cannot transfer to atom B, and atom A evolves as an excited two-level atom. For frequencies inside the photonic band gap, we have $\Gamma_{AA}(\omega) = \Gamma_{BB}(\omega) = \Gamma_{AB}(\omega) = 0$. When ω_A and ω_B are deep inside the photonic band gap, we can self-consistently determine the roots of $\Xi = 0$ [Eq. (6)]. If these roots are inside the photonic band gap, they are the discrete eigenvalues of the total Hamiltonian $H/\hbar$. This self-consistent procedure gives the exact DDI potential energy $\hbar\Delta_{AB}$, which contributes to the energy level splitting. In this situation, the linear combination of $|a\rangle$ and $|b\rangle$ forms the discrete eigenstates of the total system, which is an entangled state. In the general case where $\Gamma_{ij}(\omega) \neq 0$ and $\Delta_{ij}(\omega) \neq 0$, the singularity for the resolvent $G(\omega)$ forms a cut. Under the usual Markov approximation method where W_{ij} $(i,j = A,B)$ are independent of ω and have been replaced by $W_{ii}(\omega_i)$ and $W_{ij}[(\omega_i + \omega_j)/2]$, we are also able to determine the roots of $\Xi = 0$ [Eq. (6)]. These roots represent the unstable states of the system for the two atoms. The real part is the energy level while the imaginary part is the lifetime. Different couplings W_{ij} make the energy level splitting and the lifetime splitting different, and this is related to many novel quantum phenomena. Dipole blockade, which has been widely investigated in quantum information processing, needs a large energy gap. Efficient superradiant emission, steady-state entanglement preparation, and fast Förster energy transfer need a large lifetime splitting. However, for complex electromagnetic environments such as photonic crystals or photonic crystal nanocavities, W_{ij} may vary sharply with frequency and a non-Markov method is necessary. Also, even under the Markov approximation, the integration part of Eq. (3) is equal to the residue of these roots minus the contribution of the other part that closes the contour, which means that some corrections should be taken into account in addition to the contribution of the poles to obtain the dynamic properties. By the method described by Eq. (5), we are able to overcome the above difficulties and treat the system exactly either in the strong- or the weak-coupling regime, once we know the function of W_{ij}. Furthermore, Eq. (7) shows that all of the photonic eigenmodes contribute to the local coupling and the DDI. Equation (8c) shows that $\Delta_{ij}(\omega)$ $(i,j = A,B)$ can be obtained from $\Gamma_{ij}(\omega)$ $(i,j = A,B)$.

In the remainder of this section, we give the explicit expression for $\Gamma_{ij}(\omega)$. Insert $g_n(\mathbf{r}_i) = i\omega_i(2\varepsilon_0\hbar\omega_n)^{-1/2}\mathbf{E}_n(\mathbf{r}_i)\cdot\mathbf{u}_i$ $(i = A,B)$ into Eq. (8b) for $i \neq j$, and define $s_{i,j}(\omega) \equiv \pi\omega_i\omega_j u_i u_j/(\varepsilon_0\hbar\omega)$ $(i = A,B)$, where u_i and $\hat{\mathbf{u}}_i$ are the size and the unit vector of the transition dipole $\mathbf{u}_i$. Then we have

$$\Gamma_{ij}(\omega) = s_{i,j}(\omega)\sum_n \mathbf{E}^*_n(\mathbf{r}_i)\cdot\hat{\mathbf{u}}_i\mathbf{E}_n(\mathbf{r}_j)\cdot\hat{\mathbf{u}}_j\delta(\omega-\omega_n). \tag{9}$$

From Eqs. (2.12a) to (2.14a) of Ref. [79], it is easy to see that if $\{\mathbf{E}_n(\mathbf{r})\}$ compose a complete set of eigenmodes, $\{\mathbf{E}^*_n(\mathbf{r})\}$ are also a complete set of eigenmodes. Then Eq. (9) can also be written as

$$\Gamma_{ij}(\omega) = s_{i,j}(\omega)\sum_n \mathbf{E}_n(\mathbf{r}_i)\cdot\hat{\mathbf{u}}_i\mathbf{E}^*_n(\mathbf{r}_j)\cdot\hat{\mathbf{u}}_j\delta(\omega-\omega_n). \tag{10}$$

So we have

$$\Gamma_{ij}(\omega) = \frac{s_{i,j}(\omega)}{2}\sum_n [\mathbf{E}_n(\mathbf{r}_i)\cdot\hat{\mathbf{u}}_i\mathbf{E}^*_n(\mathbf{r}_j)\cdot\hat{\mathbf{u}}_j + \text{H.c.}]\delta(\omega-\omega_n). \tag{11}$$

Equation (11) gives the explicit expression of the local coupling strength for $i = j$ and the transfer rate for $i \neq j$ with the method of mode expansion. In the next section, we present a classical approach to obtain them without calculating the complete eigenmodes.

III. A GENERAL CLASSICAL APPROACH TO OBTAIN QUANTUM DDI

According to Eq. (11), once we know the complete eigenmodes of the electromagnetic field, we can get the transfer rate. However, it is much more difficult to obtain the complete eigenmodes for complex nanostructures. In this section, we present a classical theoretical method to rigorously calculate the DDI based on the FDTD algorithm. We will show that the transfer rate of the DDI can be analytically expressed as the difference between the two classical dipoles' total radiation power and the sum of the two individual dipole's radiation powers. In order to find this connection between the transfer rate in Eq. (11) and the emission power spectrum, we make use of the eigenmode concept to describe the radiation power spectrum. However, we need not calculate the eigenmode. The radiation power is given by the rate at which a current density source does work against a surrounding electric field or the surface integral of the normal component of the Poynting vector on the closed surface containing the dipoles. This can be directly achieved by solving the Maxwell equations with the well-known FDTD algorithm. We begin with the Maxwell equations:

$$\begin{aligned}
\nabla\times\mathbf{E}(\mathbf{r},t) &= -\frac{\partial\mathbf{B}(\mathbf{r},t)}{\partial t},\\
\nabla\times\mathbf{B}(\mathbf{r},t) &= \mu_0\varepsilon(\mathbf{r})\frac{\partial\mathbf{E}(\mathbf{r},t)}{\partial t} + \mu_0\frac{\partial\mathbf{P}(\mathbf{r},t)}{\partial t},\\
\nabla\cdot\varepsilon(\mathbf{r})\mathbf{E}(\mathbf{r},t) &= \rho(\mathbf{r},t),\\
\nabla\cdot\mathbf{B}(\mathbf{r},t) &= 0.
\end{aligned} \tag{12}$$

Expand $\mathbf{E}(\mathbf{r},t) = \sum_n \beta_n(t)\mathbf{E}_n(\mathbf{r})$ where $\mathbf{E}_n(\mathbf{r})$ are the same complete set of eigenmodes as in the quantum analysis section. If we let the polarization $\mathbf{P}(\mathbf{r},t) = e^{-i\omega_0 t}\mathbf{u}(\mathbf{r})$, then $\beta_n(t)$ satisfies the following equation:

$$\ddot{\beta_n}(t) + \omega_n^2\beta_n(t) = \omega_0^2 e^{-i\omega_0 t}\int d\mathbf{r}\mathbf{u}(\mathbf{r})\cdot\mathbf{E}^*_n(\mathbf{r}). \tag{13}$$

The solution of the above equation reads

$$\beta_n(t) = \lim_{\eta\to 0^+}\frac{\omega_0^2\exp(-i\omega_0 t)}{\omega_n^2 - (\omega_0 + i\eta)^2}\int d\mathbf{r}\mathbf{u}(\mathbf{r})\cdot\mathbf{E}^*_n(\mathbf{r}). \tag{14}$$

For $\mathbf{u}(\mathbf{r}) = \sum_i \hat{\mathbf{u}}_i\delta(\mathbf{r}-\mathbf{r}_i)$, the emission power is given by

$$P(\omega_0) = -\frac{1}{2}\text{Re}\left[\int d\mathbf{r}\frac{\partial\mathbf{P}^*(\mathbf{r},t)}{\partial t}\cdot\mathbf{E}(\mathbf{r},t)\right] \tag{15a}$$

$$= \frac{\pi}{4}\omega_0^2\sum_n\left|\sum_i\hat{\mathbf{u}}_i\cdot\mathbf{E}^*_n(\mathbf{r}_i)\right|^2\delta(\omega_0-\omega_n). \tag{15b}$$

In the case of two dipoles, i.e., $i = A, B$, the total power is

$$P^{AB}(\omega_0) = \frac{\pi}{4}\omega_0^2 \sum_n \left| \sum_{i=A,B} \hat{\mathbf{u}}_i \cdot \mathbf{E}_n^*(\mathbf{r}_i) \right|^2 \delta(\omega_0 - \omega_n). \quad (16)$$

If there is only one dipole, i.e., $i = A$ or $i = B$, then

$$P^A(\omega_0) = \frac{\pi}{4}\omega_0^2 \sum_n | \hat{\mathbf{u}}_A \cdot \mathbf{E}_n^*(\mathbf{r}_A) |^2 \delta(\omega_0 - \omega_n), \quad (17a)$$

$$P^B(\omega_0) = \frac{\pi}{4}\omega_0^2 \sum_n | \hat{\mathbf{u}}_B \cdot \mathbf{E}_n^*(\mathbf{r}_B) |^2 \delta(\omega_0 - \omega_n). \quad (17b)$$

Combining Eqs. (16), (17a), and (17b), we define the cooperative emission power as

$$\begin{aligned} P_{co}(\omega_0) &\equiv P^{AB}(\omega_0) - P^A(\omega_0) - P^B(\omega_0) \\ &= \frac{\pi\omega_0^2}{4} \sum_n [\hat{\mathbf{u}}_A \cdot \mathbf{E}_n^*(\mathbf{r}_A)\hat{\mathbf{u}}_B \cdot \mathbf{E}_n(\mathbf{r}_B) \\ &\quad + \text{H.c.}]\delta(\omega_0 - \omega_n). \end{aligned} \quad (18)$$

Comparing Eq. (18) with Eq. (11), we find

$$\frac{\Gamma_{ij}(\omega)}{\Gamma_{ii}^0(\omega)} = \frac{\mu_i \mu_j \omega_i \omega_j}{\mu_i^2 \omega_i^2} \frac{P_{co}(\omega)}{2P_0(\omega)}, \quad (19)$$

where $\Gamma_{ij}(\omega)$ is the transfer rate for $i \neq j$ and the local coupling strength for $i = j$. Correspondingly, $P_{co}(\omega)$ is the cooperative emission power of two unit classical dipoles located at different positions and the same position, respectively. $P_0(\omega)$ is the emission power of a unit classical dipole in vacuum. $\Gamma_{ii}^0(\omega)$ is the local coupling strength for a two-level atom with transition dipole moment $\mathbf{u}_i$ and transition frequency of the bare atom ω_i in vacuum.

Using the result of Ref. [8], we get $\Gamma_{ii}^0(\omega)/(u_i^2\omega_i^2) = \omega/(3\pi\varepsilon_0\hbar c^3)$. In order to determine the transfer rate more clearly, we define

$$\begin{aligned} \eta(\omega) &\equiv \frac{P_{co}(\omega)}{2P_0(\omega)}, \\ \alpha_i &\equiv \frac{u_i^2\omega_i^2}{3\pi\varepsilon_0\hbar c^3}, \end{aligned} \quad (20)$$

where α_i is totally decided by the two-level atom i. Then Eq. (19) reads

$$\Gamma_{ij}(\omega) = \sqrt{\alpha_i}\sqrt{\alpha_j}\eta(\omega)\omega. \quad (21)$$

Equation (21) is the central result of our theory. All the localized modes, guided modes, and extended modes are inherently included in the emission power spectrum. Although we have used the eigenmode concept to derive the connection between the transfer rate and the emission power spectrum, we emphasize that the complete eigenmodes need not be calculated. The emission power spectra $P_{co}(\omega)$ and $P_0(\omega)$ of the classical dipoles can be obtained from Eq. (15a) by calculating the rate at which a current density source does work against a surrounding electric field through the well-known FDTD algorithm. Once we get the transfer rate, we can obtain the DDI potential energy $\Delta_{ij}(\omega)$ through Eq. (8c). Furthermore, we find that our method may be generalized to study many-dipole interactions through a similar procedure.

IV. DDI IN A PHOTONIC CRYSTAL NANOCAVITY

In this section, the DDI in a photonic crystal (PC) nanocavity is numerically studied. A sketch of the photonic crystal cavity is displayed in Fig. 2. It consists of a thin dielectric slab with air holes arranged as a triangular lattice. The lattice constant is a, the radius of the air holes is $r = 0.3a$, and the slab height is $d = 0.6a$. The refractive index of the slab is 3.4. There is a defect hole in the center with refractive index $n_{\text{def}} = 2.4$. Its radius is the same as that of the air holes. The two dipoles are located at points A and B on the center plane of the slab, and the two transition dipole moments are parallel to the x axis. The origin of the axes is set at the center of the PC cavity. For convenience, the special points are also drawn in Fig. 2. Atom A is located at $(0, -11/15, 0)a$ and atom B at $(0, R - 11a/15, 0)$, where R represents the separation and varies from $a/15$ to $50a/15$. The two transition dipole moments are parallel to the x axis. Thanks to the scaling law, the transfer rate $\Gamma_{ij}(\omega)$, dipole-dipole interaction potential energy $\Delta_{ij}(\omega)$, and frequency ω in units of $2\pi c/a$ are dimensionless.

The frequency-dependent characteristics for the transfer rate $\Gamma_{ij}(\omega)$ and the DDI potential energy $\Delta_{ij}(\omega)$ are presented in Figs. 3(a) and 3(b) for atom A located at $(0, -11/15, 0)a$ and atom B located at $(0, 11/15, 0)a$. Γ_{ij} and $\mathbf{\Delta}_{ij}$ are in units of α_{ij} ($\alpha_{ij} \equiv \sqrt{\alpha_i}\sqrt{\alpha_j}2\pi c/a$). The insets show the behaviors for frequency around the resonance frequency [$\omega_c = 0.3133(2\pi c/a)$]. From Fig. 3(a), we clearly see that $\Gamma_{ij}(\omega)$ oscillates remarkably when ω is far away from ω_c, which shows the powerful modulation ability of the photonic crystal for the electromagnetic eigenmode and the density of photonic states. For $\omega = \omega_c$ (inset), $\Gamma_{ij}(\omega_c) \approx 144\Gamma_0$ for a relatively large atomic separation ($R \approx 0.46\lambda_0$), where λ_0 is the resonance wavelength of the cavity and Γ_0

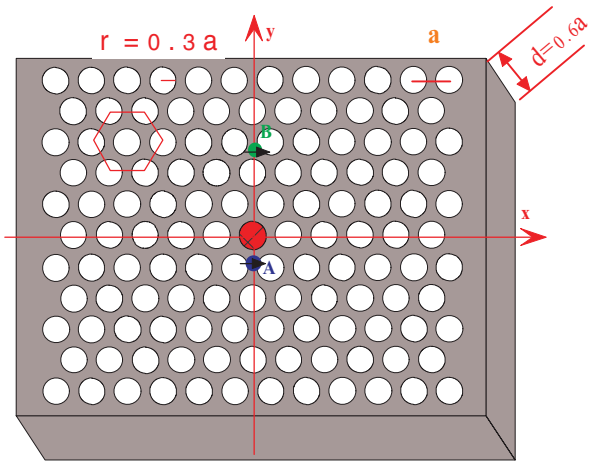

FIG. 2. (Color online) Sketch of the photonic crystal nanocavity. It consists of a thin dielectric slab with air holes arranged as a triangular lattice. The lattice constant is a, the radius of the air holes is $r = 0.3a$, and the slab height is $d = 0.6a$. The refractive index of the slab is 3.4. There is a defect hole in the center with refractive index $n_{\text{def}} = 2.4$. Its radius is the same as that of the air holes. The origin of the axes is set at the center of the photonic crystal nanocavity. The two dipoles are located at points A and B on the center plane of the slab, and the two transition dipole moments are parallel to the x axis.

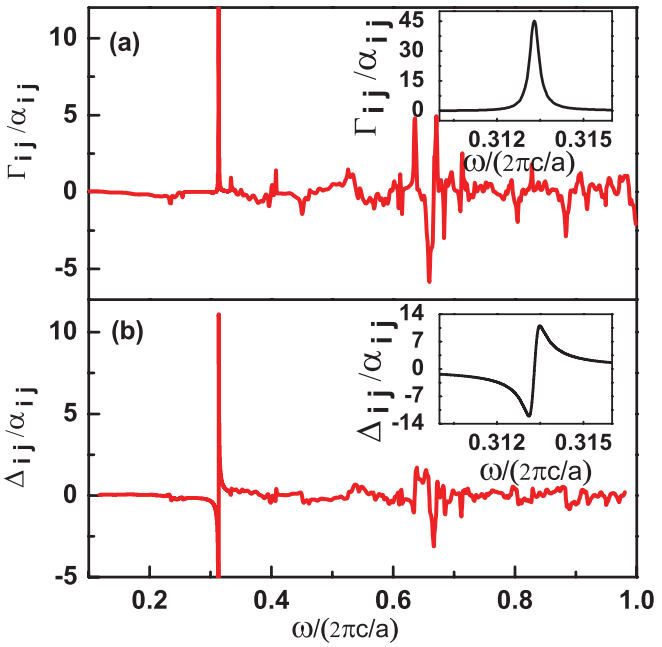

FIG. 3. (Color online) Frequency-dependent characteristics for the transfer rate and the DDI potential energy. (a) The transfer rate $\Gamma_{ij}(\omega)$ and (b) the DDI potential energy $\Delta_{ij}(\omega)$ versus ω for atom A located at $(0, -11/15,0)a$ and atom B located at $(0,11/15,0)a$ in the photonic crystal nanocavity. $\Gamma_{ij}(\omega)$ and $\Delta_{ij}(\omega)$ are in units of α_{ij} ($\alpha_{ij} \equiv \sqrt{\alpha_i}\sqrt{\alpha_j}2\pi c/a$). The frequency ω is in units of $2\pi c/a$. The two dipole moments are parallel and along the x axis. The insets show the behavior around the defect frequency [$\omega_c = 0.3133(2\pi c/a)$] of the cavity. The two transition dipoles are parallel and along the x axis.

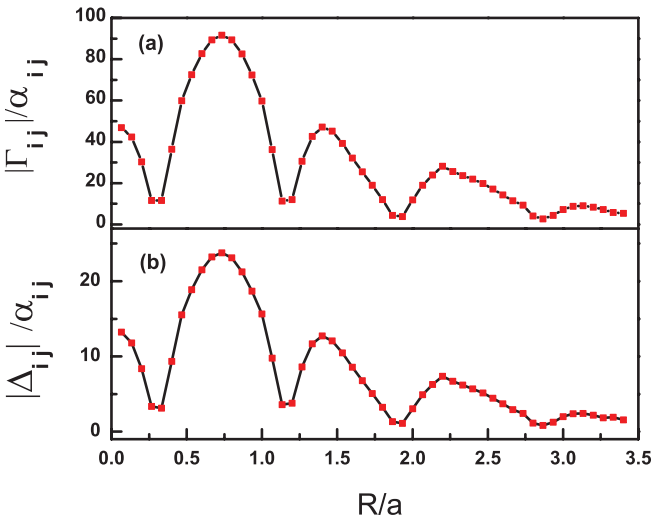

FIG. 4. (Color online) Position-dependent properties for the transfer rate and the DDI potential energy. (a) The absolute maximum transfer rate $|\Gamma_{ij}|$ and (b) the absolute maximum DDI potential energy $|\mathbf{\Delta}_{ij}|$ versus the interatomic separation R for atom A located at $(0, -11/15,0)a$ and atom B located at $(0, R - 11a/15,0)$ in the PC cavity. The maxima are taken for ω around ω_c. $|\Gamma_{ij}|$ and $|\mathbf{\Delta}_{ij}|$ are in units of α_{ij} ($\alpha_{ij} \equiv \sqrt{\alpha_i}\sqrt{\alpha_j}2\pi c/a$). The atomic separation is in units of the lattice constant a. The two transition dipoles are parallel and along the x axis.

is the largest $\Gamma_{ij}(\omega_c)$ for two dipoles located in vacuum with the atomic separation $R = 0$. This large Γ_{ij} is attributed to the enhancement of the photon emission and reabsorbance rates, which can be roughly characterized by the ratio Q/V. Aiming at quantum computation and quantum information processing [59,60], where large Γ_{ij} or large $\mathbf{\Delta}_{ij}$ is needed, we can increase the quality factor Q through improving the nanocavity design. For $\omega \sim \omega_c$ (inset), $\Gamma_{ij}(\omega)$ varies sharply and is sensitive to the frequency, which implies that tuning ω_c of the cavity or ω_i of the dipole can both help to control Γ_{ij}. Figure 3(b) shows similar properties for the DDI potential energy. The inset shows that a repulsive or an attractive potential energy can be obtained around the resonance frequency of the cavity.

The position-dependent properties have also been investigated. Figures 4(a) and 4(b) show the absolute maximum values of the transfer rate $|\Gamma_{ij}|$ and the DDI potential energy $|\mathbf{\Delta}_{ij}|$ as a function of the atom separation R [atom A located at $(0, -11a/15,0)$ and atom B located at $(0, R - 11a/15,0)$], where the maxima are calculated for ω around ω_c. $|\Gamma_{ij}|$ and $|\mathbf{\Delta}_{ij}|$ are also in units of α_{ij}. The atomic separation is in units of the lattice constant a. The maximum values of $|\Gamma_{ij}|$ and $|\mathbf{\Delta}_{ij}|$ vary in a similar way except for the amplitude. The above phenomena can be understood as follows: $|\Gamma_{ij}|$ depends greatly on the electric field of the defect mode. Equation (11) shows that $|\Gamma_{ij}|$ changes in the same way as the electric field of the cavity mode at the location of atom B. The cavity mode along the y axis looks the same as Fig. 4(a) and we do not show it here. Further, we clearly see that $|\Gamma_{ij}| = |\Gamma_{ii}|$ and $|\mathbf{\Delta}_{ij}| = |\mathbf{\Delta}_{ii}|$ have been realized for atom A and atom B located at positions along the x axis with the same electric field strength.

V. CONCLUSION

In summary, we have proposed a rigorous numerical method to investigate DDI in a photonic crystal nanocavity. We need not calculate the eigenmode. The transfer rate of the DDI is analytically expressed as the difference between the two classical dipoles' total radiation power and the sum of the two individual dipole's radiation powers [Eq. (21)], which is the central result of our theory. The radiation power is obtained from Eq. (15a) by calculating the rate at which a current density source does work against a surrounding electric field. This has been achieved by directly solving the Maxwell equations in real space with a free-space boundary condition through the well-known FDTD algorithm. Utilizing Eq. (8c), we have obtained the DDI potential energy. Further, the method can be applied for dipoles with different transition frequencies in both the weak- and strong-coupling regimes. It works well for dipoles located in photonic nanostructures with arbitrary shape and can be generalized to calculate many-dipole interactions.

We have applied this theory to investigate the DDI in a photonic crystal nanocavity. It is found that the transfer rate and the potential energy of the DDI strongly depend on the atomic transition frequency, the atomic position, the resonance frequency, and the quality factor of the cavity. A large transfer rate at a distance has been achieved under resonant conditions

and with a high quality factor. Equal values of the transfer rate and the local coupling strength have been obtained for two equal dipoles located at proper positions. Attractive or repulsive properties of the DDI potential energy have been obtained around the resonance frequency. Our results should be significant for solid-state quantum information processing based on the DDI.

ACKNOWLEDGMENTS

This work was financially supported by the National Basic Research Program of China (Grants No. 2010CB923200 and No. 2011CB921502) and the National Natural Science Foundation of China (Grants No. 10725420, No. U0934002, and No.10934010).

[1] E. M. Purcell, Phys. Rev. **69**, 681 (1946).
[2] G. Barton, Proc. R. Soc. London, Ser. A **320**, 251 (1970).
[3] G. S. Agarwal, Phys. Rev. A **12**, 1475 (1975).
[4] R. G. Hulet, E. S. Hilfer, and D. Kleppner, Phys. Rev. Lett. **55**, 2137 (1985).
[5] S. John, Phys. Rev. Lett. **58**, 2486 (1987).
[6] H. Yokoyama, Science **256**, 66 (1992).
[7] S. Scheel, L. Knöll, D. G. Welsch, and S. M. Barnett, Phys. Rev. A **60**, 1590 (1999).
[8] X. H. Wang, B. Y. Gu, R. Z. Wang, and H. Q. Xu, Phys. Rev. Lett. **91**, 113904 (2003).
[9] T. Yoshie, A. Scherer, J. Hendrickson, G. Khitrova, H. M. Gibbs, G. Rupper, C. Ell, O. B. Shchekin, and D. G. Deppe, Nature (London) **432**, 200 (2004).
[10] S. M. Thon, M. T. Rakher, H. Kim, J. Gudat, W. T. M. Irvine, P. M. Petroff, and D. Bouwmeester, Appl. Phys. Lett. **94**, 111115 (2009).
[11] M. L. Andersen, S. Stobbe, A. S. Søensen, and P. Lodahl, Nat. Phys. **7**, 215 (2011).
[12] G. Khitrova, H. M. Gibbs, M. Kira, S. W. Koch, and A. Scheerer, Nat. Phys. **2**, 81 (2006).
[13] K. M. Birnbaum, A. Boca, R. Miller, A. D. Boozer, T. E. Northup, and H. J. Kimble, Nature (London) **436**, 87 (2005).
[14] M. J. Hartmann, F. G. S. L. Brandão, and M. B. Plenio, Nat. Phys. **2**, 849 (2006).
[15] A. D. Greentree, C. Tahan, J. H. Cole, and L. C. L. Hollenberg, Nat. Phys. **2**, 856 (2006).
[16] P. Goy, J. M. Raimond, M. Gross, and S. Haroche, Phys. Rev. Lett. **50**, 1903 (1983).
[17] H. Walther, B. T. H. Varcoe, B. G. Englert, and T. Becker, Rep. Prog. Phys. **69**, 1325 (2006).
[18] D. Braun, Phys. Rev. Lett. **89**, 277901 (2002).
[19] K. Panajotov and M. Dems, Opt. Lett. **35**, 829 (2010).
[20] D. Meschede, H. Walther, and G. Muller, Phys. Rev. Lett. **54**, 551 (1985).
[21] O. Painter, R. K. Lee, A. Scherer, A. Yariv, J. D. Dapkus, J. D. O'Brien, and I. Kim, Science **284**, 1819 (1999).
[22] S. Noda, Science **314**, 260 (2006).
[23] R. H. Lehmberg, Phys. Rev. A **2**, 883 (1970).
[24] G. S. Agarwal and A. K. Patnaik, Phys. Rev. A **63**, 043805 (2001).
[25] C. Hettich, C. Schmitt, J. Zitzmann, S. Kühn, I. Gerhardt, and V. Sandoghdar, Science **298**, 385 (2002).
[26] H. Y. Lu, H. Lu, J. N. Zhang, R. Z. Qiu, H. Pu, and S. Yi, Phys. Rev. A **82**, 023622 (2010)
[27] E. V. Goldstein and P. Meystre, Phys. Rev. A **56**, 5135 (1997).
[28] T. Kobayashi, Q. B. Zheng, and T. Sekiguchi, Phys. Rev. A **52**, 2835 (1995).
[29] R. H. Lehmberg, Phys. Rev. A **2**, 889 (1970).
[30] G. S. Agarwal and S. DuttaGupta, Phys. Rev. A **57**, 667 (1998).
[31] S. Rist, J. Eschner, M. Hennrich, and G. Morigi, Phys. Rev. A **78**, 013808 (2008).
[32] L. M. Folan. S. Arnold, and S. D. Druger, Chem. Phys. Lett. **118**, 322 (1985).
[33] S. Bay, P. Lambropoulos, and K. Mølmer, Phys. Rev. A **55**, 1485 (1997).
[34] P. T. Kristensen, J. Mørk, P. Lodahl, and S. Hughes, Phys. Rev. B **83**, 075305 (2011).
[35] E. Gallardo, L. J. Martínez, A. K. Nowak, D. Sarkar, H. P. van der Meulen, J. M. Calleja, C. Tejedor, I. Prieto, D. Granados, A. G. Taboada, J. M. García, and P. A. Postigo, Phys. Rev. B **81**, 193301 (2010).
[36] A. Laucht, J. M. Villas-Bôas, S. Stobbe, N. Hauke, F. Hofbauer, G. Böhm, P. Lodahl, M. C. Amann, M. Kaniber, and J. J. Finley, Phys. Rev. B **82**, 075305 (2010).
[37] S. Reitzenstein, A. Loeffler, C. Hofman, A. Kubanek, M. Kamp, J. P. Reithmaier, and A. Forchel, Opt. Lett. **31**, 1738 (2006).
[38] S. Weiler, A. Ulhaq, S. M. Ulrich, S. Reitzenstein, A. Loffler, A. Forchel, and P. Michler, Phys. Rev. B **82**, 205326 (2010).
[39] H. Kim, D. Sridharan, T. C. Shen, G. S. Solomon, and E. Waks, Opt. Express **19**, 2589 (2011).
[40] A. Gonzalez-Tudela, D. Martin-Cano, E. Moreno, L. Martin-Moreno, C. Tejedor, and F. J. Garcia-Vidal, Phys. Rev. Lett. **106**, 020501 (2011).
[41] F. Zhou, Y. Liu, and Z. Y. Li, Opt. Lett. **36**, 1969 (2011).
[42] D. Dzsotjan, J. Kästel, and M. Fleischhauer, Phys. Rev. B **84**, 075419 (2011).
[43] D. Dzsotjan, A. S. Sørensen, and M. Fleischhauer, Phys. Rev. B **82**, 075427 (2010).
[44] D. M. Cano, L. M. Moreno, F. J. G. Vidal, and E. Moreno, Nano Lett. **10**, 3129 (2010).
[45] Y. P. Yang, J. P. Xu, H. Chen, and S. Y. Zhu, Phys. Rev. A **82**, 030304(R) (2010).
[46] J. Xu, M. Al-Amri, Y. Yang, S. Y. Zhu, and M. S. Zubairy, Phys. Rev. A **84**, 032334 (2011).
[47] Y. Takahashi, H. Hagino, Y. Tanaka, B. Song, T. Asano, and S. Noda, Opt. Express **15**, 17206 (2007).
[48] Y. Tanaka, T. Asano, and S. Noda, J. Lightwave Technol. **26**, 0733 (2008).
[49] S. Vignolini, F. Intonti, F. Riboli, L. Balet, L. H. Li, M. Francardi, A. Gerardino, A. Fiore, D. S. Wiersma, and M. Gurioli, Phys. Rev. Lett. **105**, 123902 (2010).
[50] S. Mosor, J. Hendrickson, B. C. Richards, J. Sweet, G. Khitrova, H. M. Gibbs, T. Yoshie, A. Scherer, O. B. Shchekin, and D. G. Deppe, Appl. Phys. Lett. **87**, 141105 (2005).
[51] M. Burresi, T. Kampfrath, D. van Oosten, J. C. Prangsma, B. S. Song, S. Noda, and L. Kuipers, Phys. Rev. Lett. **105**, 123901 (2010).

[52] Y. Tanaka, J. Upham, T. Nagashima, T. Sugiya, T. Asano, and S. Noda, Nat. Mater. **6**, 862 (2007).
[53] T. Tanabe, M. Notomi, H. Taniyama, and E. Kuramochi, Phys. Rev. Lett. **102**, 043907 (2009).
[54] K. D. Jöns, R. Hafenbrak, R. Singh, F. Ding, J. D. Plumhof, A. Rastelli, O. G. Schmidt, G. Bester, and P. Michler, Phys. Rev. Lett. **107**, 217402 (2011).
[55] A. Faraon, A. Majumdar, H. Kim, P. Petroff, and J. Vučković, Phys. Rev. Lett. **104**, 047402 (2010).
[56] S. Reitzenstein, S. Münch, P. Franeck, A. Rahimi-Iman, A. Löffler, S. Höfling, L. Worschech, and A. Forchel, Phys. Rev. Lett. **103**, 127401 (2009).
[57] S. Karaveli and R. Zia, Phys. Rev. Lett. **106**, 193004 (2011).
[58] M. D. Lukin and P. R. Hemmer, Phys. Rev. Lett. **84**, 2818 (2000).
[59] M. D. Lukin, M. Fleischhauer, R. Cote, L. M. Duan, D. Jaksch, J. I. Cirac, and P. Zoller, Phys. Rev. Lett. **87**, 037901 (2001).
[60] D. Jaksch, J. I. Cirac, P. Zoller, S. L. Rolston, R. Cote, and M. D. Lukin, Phys. Rev. Lett. **85**, 2208 (2000).
[61] L. Isenhower, E. Urban, X. L. Zhang, A. T. Gill, T. Henage, T. A. Johnson, T. G. Walker, and M. Saffman, Phys. Rev. Lett. **104**, 010503 (2010).
[62] S. B. Zheng and G. C. Guo, Phys. Rev. Lett. **85**, 2392 (2000).
[63] S. Hughes, Phys. Rev. Lett. **94**, 227402 (2005).
[64] P. Yao and S. Hughes, Opt. Express **17**, 11505 (2009).
[65] A. Gonzalez-Tudela, D. Martin-Cano, E. Moreno, L. Martin-Moreno, C. Tejedor, and F. J. Garcia-Vidal, Phys. Rev. Lett. **106**, 020501 (2011).
[66] J. Ruostekoski and J. Javanainen, Phys. Rev. A **55**, 513 (1997).
[67] H. Y. Xie, H. Y. Chung, P. T. Leung, and D. P. Tsai, Phys. Rev. B **80**, 155448 (2009).
[68] Y. K. Youl, C. K. Cheol, and A. C. Won, Opt. Express **17**, 11495 (2009).
[69] I. E. Protsenko, A. V. Uskov, O. A. Zaimidoroga, V. N. Samoilov, and E. P. O'Reilly, Phys. Rev. A **71**, 063812 (2005).
[70] A. Reinhard, K. C. Younge, T. C. Liebisch, B. Knuffman, P. R. Berman, and G. Raithel, Phys. Rev. Lett. **100**, 233201 (2008).
[71] T. A. Johnson, E. Urban, T. Henage, L. Isenhower, D. D. Yavuz, T. G. Walker, and M. Saffman, Phys. Rev. Lett. **100**, 113003 (2008).
[72] N. Saquet, A. Cournol, J. Beugnon, J. Robert, P. Pillet, and N. Vanhaecke, Phys. Rev. Lett. **104**, 133003 (2010).
[73] M. Harlander, R. Lechner, M. Brownnutt, R. Blatt, W. Hänsel, Nature (London) **471**, 200 (2011)
[74] M. H. G. de Miranda, A. Chotia1, B. Neyenhuis, D. Wang, G. Quéméner, S. Ospelkaus, J. L. Bohn, J. Ye, and D. S. Jin, Nat. Phys. **7**, 502 (2011).
[75] S. I. Schmid and J. Evers, Phys. Rev. A **77**, 013822 (2008).
[76] M. Wubs, L. G. Suttorp, and A. Lagendijk, Phys. Rev. A **70**, 053823 (2004).
[77] W. H. Louisell, *Quantum Statistical Properties of Radiation* (John Wiley & Sons, New York, 1973).
[78] C. C. Tannoudji, J. D. Poc, and G. Grynberg, *Atom-Photon Interactions: Basic Processes and Application* (John Wiley & Sons, New York, 1992).
[79] R. J. Glauber and M. Lewenstein, Phys. Rev. A **43**, 467 (1991).